

## Radiative Capture to Unbound States via a Bremsstrahlung Mechanism

Dean Halderson and R. J. Philpott

*Department of Physics, The Florida State University, Tallahassee, Florida 32306*

(Received 8 January 1980; revised manuscript received 20 November 1980)

Observations of intermediate-energy proton capture populating unbound states are analyzed in terms of the bremsstrahlung emitted during single-particle transitions. The model accounts for the major features of the data. The present results suggest that these experiments can yield information on the structure of highly excited states.

PACS numbers: 25.40.Lw, 24.10.-i

Capture measurements<sup>1</sup> to excited nuclear states have been of recent interest because they may be used to observe giant resonances built on these excited states and to gain information on particle unbound states for which ground-state transitions are inhibited due, for example, to large angular-momentum differences. Of particular interest are the measurements of Kovash *et al.*<sup>2</sup> and Blatt *et al.*<sup>3</sup> In the reactions  $^{11}\text{B}(p, \gamma)$ ,  $^{12}\text{C}(p, \gamma)$ , and  $^{27}\text{Al}(p, \gamma)$  at incident proton energies of  $\sim 40$  MeV, distinct peaks were observed in the  $\gamma$ -ray spectrum. Most of these peaks correspond to excitation energies of the compound nucleus which are above proton threshold. Moreover, the peaks essentially disappear at higher bombarding energies.

It was suggested in Ref. 2 that these peaks could be characteristic of "second-harmonic giant resonances" which may be construed as requiring a collective origin. But Arnold<sup>4</sup> has argued that the transitions are primarily single particle in na-

ture. Tsai and Londergan<sup>5</sup> have performed a calculation with bound one-particle, one-hole (1p-1h) states which require certain "exchange currents" to reproduce the observed cross sections in  $^{11}\text{B}(p, \gamma)$ .

Since the reactions discussed in Refs. 2 and 3 lead to particle unbound final states, it is appropriate to develop a model which treats them as such. The present paper describes the results of calculations for the bremsstrahlung emitted by a proton undergoing a continuum-to-continuum transition while interacting with the target nucleus via a phenomenological potential of standard form. This model can then be used to determine to what extent the single-particle theory is sufficient to describe the experimental data. The present results show that the single-particle mechanism can account for the major features of the observations.

The bremsstrahlung calculations are based on the following standard expression<sup>6</sup> for the cross section:

$$\frac{d^2\sigma}{d\Omega dE} = \frac{1}{(2\pi\hbar)^4} \frac{E}{\hbar cv_i} \int d^3p_1' \int d^3p_2' |\langle \psi_f^{(-)} | H_e(\vec{k}, \vec{\epsilon}) | \psi_i^{(+)} \rangle|^2 \delta(E_f - E_i) \delta(\vec{P}_f - \vec{P}_i), \quad (1)$$

where  $E$  is the energy of the observed photon,  $v_i$  is the relative velocity in the incident channel, and  $\vec{p}_1'$  and  $\vec{p}_2'$  are the momenta of the scattered proton and recoiling nucleus. The exponentially normalized wave functions  $\psi_i^{(+)}$  and  $\psi_f^{(-)}$  are those of the initial and final nuclear states, and  $H_e(\vec{k}, \vec{\epsilon})$  represents the electromagnetic interaction in the notation of Rose and Brink.<sup>7</sup> The above expression does not exhibit sums and averages over final- and initial-spin projections, which will be included below.

For the calculations reported here, the nuclear wave functions are represented by optical-model wave functions with partial-wave decomposition

$$\psi_{\vec{k}, m_s}^{(\pm)} = \sum_{l, m_l, j, m} Y_{lm_l}^*(\hat{k}) \langle l m_l \frac{1}{2} m_s | j m \rangle \psi_{l j m}^{(\pm)}, \quad (2)$$

where  $\langle l m_l \frac{1}{2} m_s | j m \rangle$  is a Clebsch-Gordan coefficient. Also the electromagnetic interaction is limited to the dominant spin-independent electric dipole and quadrupole terms. Equation (1) can now be re-

duced quite straightforwardly to the form

$$\frac{d^2\sigma}{d\Omega dE} = \frac{m_f p_f}{(2\pi\hbar)^5} \frac{E}{2c v_i} \sum_j C_j P_j(\cos\theta), \quad (3)$$

$$C_j = \sum_{\substack{l', j', l'', j'' \\ l, l', l'', l'''}} (-1)^{L+J+1/2} \hat{l} \hat{l}'' \hat{j} \hat{j}'' [j'] \langle L, -1, L', 1 | J, 0 \rangle \langle l, 0, l'', 0 | J, 0 \rangle \\ \times W(l, l'', j, j''; J, \frac{1}{2}) W(j', j'', L, J; L', j) \tau_L(l', j'; l, j) \tau_{L'}^*(l'', j''; l'', j'') [1 + (-1)^{L+L'-J}]/2. \quad (4)$$

In the above the  $\tau_L(l', j'; l, j)$  are reduced partial-wave transition-matrix elements given by  $\tau_L(l', j'; l, j) = \langle \psi_{l', j', (-)} | | T_{LM}^{(e)} | | \psi_{l, j, (+)} \rangle$ . The  $T_{LM}^{(e)}$  operators contain both a proton and target-nucleus contribution, thus accounting for target recoil. In the notation of Rose and Brink,<sup>7</sup> the operators are written as

$$T_{LM}^{(e)} = \sum \{ (2L+1) / [2L(L+1)]^{1/2} \} i^L (2\beta Z_n / i k A_n) \{ \{ k^2 \vec{r}_n + \nabla_n [ j_L(kr_n) + k r_n j_{L'}(kr_n) ] C_{LM}(\hat{r}_n) \} \cdot \vec{p}_n, \quad (5)$$

where  $(\vec{r}_1, \vec{r}_2) = [m_2 \vec{r} / (m_1 + m_2), -m_1 \vec{r} / (m_1 + m_2)]$ , and  $(\vec{p}_1, \vec{p}_2) = (\vec{p}, -\vec{p}) = (-i \nabla_r, i \nabla_r)$ . The operators  $\vec{r}$  and  $\vec{p}$  are the relative coordinate and associated momentum, and  $m_f$  and  $p_f$  are the values of the reduced mass and relative momentum in the final proton-nucleus system. Standard angular-momentum notation<sup>8</sup> is employed.

The geometry of all potential wells was fixed by the parameters,  $r_i = 1.25$  and  $a_i = 0.55$ . Spin-orbit and surface-absorption terms are employed as determined by Kolata and Galonsky<sup>9</sup> from fits to elastic proton scattering on <sup>12</sup>C at  $E_p^{\text{lab}} = 40$  MeV. The real well depth was then adjusted to provide a fit to elastic scattering at various energies. A linear energy dependence was assumed for the potential depths.

At the excitation energy of the compound nucleus corresponding to the exit-proton energy, there are many resonances. The elastic proton scattering is dominated by the resonances. Therefore the real potential and spin-orbit depths were adjusted to best reproduce these resonance positions. Reasonable fits to elastic proton scattering are then obtained. The well parameters for all energy ranges are given in Table I.

The data for <sup>12</sup>C( $p, \gamma$ ) at  $E_p^{\text{lab}} = 40$  MeV are shown in Fig. 1(a). The peaks have been labeled I-V for reference. Peak I corresponds to transitions to the particle-bound ground state of <sup>13</sup>N. Peak II overlaps transitions to  $\frac{1}{2}^+$ ,  $\frac{3}{2}^-$ , and  $\frac{5}{2}^+$

proton-unstable final states. Peak III aligns with transitions to the  $E_x = 7.9$  MeV,  $\frac{3}{2}^+$  state. Three optical-model single-particle resonances corresponding to the  $\frac{1}{2}^+$ ,  $\frac{5}{2}^+$ , and  $\frac{3}{2}^+$  states were placed at the appropriate energies with the parameters shown in Table I. All partial waves with  $l \leq 8$  were included in the entrance and exit channels. The results of the calculation are represented as a solid line in Fig. 1(a) after energy averaging with a Gaussian of 2.5 MeV full width at half maximum to simulate the detector resolution. The arrow indicates proton threshold.

Peak II is the first peak that should be described by the present model. The calculation does well at producing the observed strength. As one goes to lower  $\gamma$ -ray energy, the comparison of theory with experiment becomes difficult since there is an increasingly large background, some of which is due to inelastic ( $p, p' \gamma$ ) processes. A lower limit for the background can be constructed by fitting a Lorentzian curve to the first identified inelastic peak. This curve is shown as a dot-dashed line in Fig. 1. Inclusion of just this minimal background brings peak III into reasonable agreement with experiment. From the experimental spectrum<sup>10</sup> of <sup>13</sup>N, there are also large concentrations of  $l=2$  strength at the excitation energies corresponding to peaks IV and V; however, the optical model, which does not allow for

TABLE I. Woods-Saxon well parameters.

Channel	Target	Energy range $E_p$ (MeV)	$V_0$	$W_D$	$W_{s.o.}$
Incident	<sup>12</sup> C, <sup>11</sup> B	10-80	46 - 0.2E	3.19 - 0.05E	6.26 - 0.01E
Exit	<sup>12</sup> C	0-10.2	58.2	0	4.70
Exit	<sup>11</sup> B	0-11.3	57.7	0	3.96

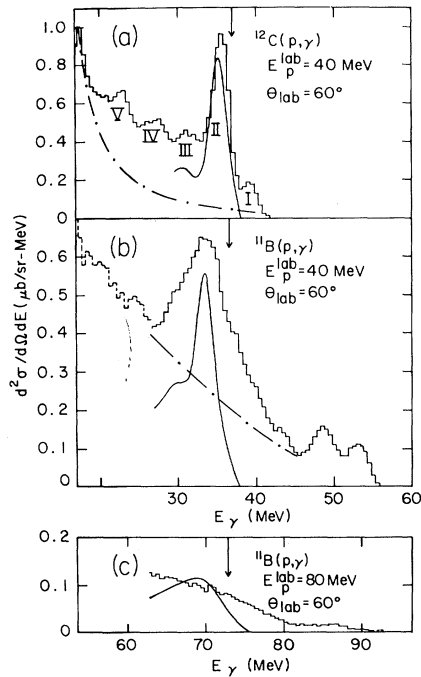


FIG. 1. Photon cross sections. Histograms are data of Ref. 2. Smooth solid curves are theory. Dot-dashed lines represent backgrounds as explained in the text. The arrow indicates proton threshold.

fragmentation of single-particle levels, would produce widths which are too large for describing these states.

In  $^{11}\text{B}(p, \gamma)$ , the single-particle states are fragmented among spin multiplets. However, the strength is still reasonably well concentrated.<sup>11</sup> Therefore the same procedure as followed for  $^{12}\text{C}(p, \gamma)$  is applied to  $^{11}\text{B}(p, \gamma)$  and three resonances,  $s_{1/2}$ ,  $d_{5/2}$ , and  $d_{3/2}$  are placed at  $E_p^{\text{lab}} = 1.0, 3.9, \text{ and } 8.5$  MeV, respectively. Unfortunately elastic-proton-scattering data at 40 MeV are not available at the present time, and so the choice of a potential depth is uncertain. As a reasonable estimate, the  $^{12}\text{C} + p$  potential was employed.

Figure 1(b) shows the  $E_p^{\text{c.m.}} = 40$  MeV results for  $^{11}\text{B} + p$ . Although not evident from the initial measurements, the large peak at  $E_\gamma \sim 33$  MeV sits atop a large background. This can be seen from the new measurement at  $E_p^{\text{c.m.}} = 50$  MeV, which has been included as a dashed histogram in Fig. 1(b), shifted by  $E_\gamma = 9.2$  MeV and normalized to the 40-MeV data at  $E_\gamma = 27$  MeV. In this case even less knowledge of the background is available. It can be said, however, that there is enough strength under the calculated solid curve to ac-

count for the experimental strength above the dot-dashed line.

Figure 1(c) displays the experimental  $^{11}\text{B}(p, \gamma)$  cross section at  $E_p^{\text{lab}} = 80$  MeV. The detector resolution has been assumed proportional to  $E_\gamma$  and therefore the 80-MeV calculation has been folded with a Gaussian of 5 MeV width. Again a proper knowledge of the 80-MeV optical potential is lacking, but these results with the  $^{12}\text{C} + p$  energy-dependent potential do demonstrate that, as with the data, the calculated cross section drops at higher proton energies. This is because there is less preferential overlap of the incident partial waves with the resonant exit partial wave in the electromagnetic transition-matrix elements.

In conclusion, bremsstrahlung emitted in single-particle transitions is capable of reproducing the observed features of intermediate-energy proton capture to unbound states. Enhancement due to "exchange currents" or collective behavior do not appear necessary. The experiments are extremely interesting even in the light of our present interpretation, because they provide valuable information on the wave functions of highly excited states which is not attainable from particle scattering experiments. Finally, we remark that the use of a single-particle-potential model is, of course, very restrictive and cannot be expected to reproduce all observed effects. Calculations with appropriate additional degrees of freedom should be pursued in the future as well as further experiments which can test these calculations.

This work was supported in part by the National Science Foundation.

<sup>1</sup>S. H. Chew, J. Lowe, and J. M. Nelson, Nucl. Phys. **A286**, 451 (1977), and references therein.

<sup>2</sup>M. A. Kovash, S. L. Blatt, R. N. Boyd, T. R. Donoghue, H. J. Hausman, and A. D. Bacher, Phys. Rev. Lett. **42**, 700 (1979).

<sup>3</sup>S. L. Blatt, M. A. Kovash, T. R. Donoghue, R. N. Boyd, H. J. Hausman, and A. D. Bacher, Bull. Am. Phys. Soc. **24**, 843 (1979).

<sup>4</sup>L. G. Arnold, Phys. Rev. Lett. **42**, 1253 (1979).

<sup>5</sup>S.-F. Tsai and J. T. Londergan, Phys. Rev. Lett. **43**, 576 (1979).

<sup>6</sup>R. G. Newton, *Scattering Theory of Particles and Waves* (McGraw-Hill, New York, 1967).

<sup>7</sup>H. J. Rose and D. M. Brink, Rev. Mod. Phys. **39**, 306 (1967).

<sup>8</sup>M. E. Rose, *Elementary Theory of Angular Momentum* (Wiley, New York, 1957).

<sup>9</sup>J. J. Kolata and A. Galonsky, *Phys. Rev.* **182**, 1073

(1969).

<sup>10</sup>F. Ajzenberg-Selove, *Nucl. Phys.* **A268**, 1 (1976).

<sup>11</sup>D. Halderson and R. J. Philpott, to be published.

## Nuclear-Structure Effects Connected with Charge-Exchange Resonances

S. Krewald and F. Osterfeld

*Institut für Kernphysik, Kernforschungsanlage Jülich, D-5170 Jülich, West Germany*

and

J. Speth<sup>(a)</sup> and G. E. Brown

*Department of Physics, State University of New York, Stony Brook, New York 11794*

(Received 25 August 1980)

The excitation energies and the  $(p, n)$  cross sections of the giant Gamow-Teller resonance as well as the isobaric analog state in  $^{208}\text{Pb}$  are calculated. Similar to the results in electron scattering, the theoretical spin-flip strength overestimates the experimental one appreciably. The excitation energies of the spin-dependent excitations and the isobaric analog resonance can only be explained simultaneously if the effects of the "dynamical theory of collective states" and of the one-pion- and one- $\rho$ -exchange potential are taken into account.

PACS numbers: 21.10.Pc, 21.60.Jz, 25.30.Cq

Using a highly energetic proton beam, Goodman *et al.*<sup>1,2</sup> recently obtained detailed experimental results on the Gamow-Teller resonances (GTR) in many nuclei. These  $1^+$  resonances which have been reported<sup>3</sup> earlier in  $^{90}\text{Zr}$  turned out to be the dominant reaction channel in a high-energy  $(p, n)$  reaction at very forward angles. The structure of these states is very similar to the well-known isobaric analog states (IAR). Both resonances can be described in the framework of the random-phase approximation (RPA) theory as a superposition of proton-particle, neutron-hole states.<sup>4,5</sup> In the case of the IAR the particle-hole pairs are coupled to  $0^+$ , in the GTR case to  $1^+$ . Both kinds of states are expected to be rather collective in heavy-mass nuclei.

In the following we investigate the situation in  $^{208}\text{Pb}$ . With a  $(p, n)$  reaction one excites, in this case, states in  $^{208}\text{Bi}$ . In order to obtain the structure of these resonances one has to solve the

RPA equation:

$$\chi_{12}^{\mu} = \frac{n_1 - n_2}{\epsilon_1 - \epsilon_2 - \Omega_{\mu}} \sum_{3,4} F_{14,23}^{p-h} \chi_{34}^{\mu}. \quad (1)$$

The amplitudes  $\chi^{\mu}$  are connected with the scattering cross section and  $\Omega_{\mu}$  is the excitation energy of the corresponding state  $\mu$ . In order to solve Eq. (1) one needs single-particle energies  $\epsilon_{\nu}$  and a particle-hole interaction  $F^{p-h}$ . The  $n_{\nu}$  denote the occupation probability 0 or 1 of a given single-particle state  $\nu$ .

Since the levels excited by a  $(p, n)$  reaction are connected with a change in isospin, they allow a selective investigation of the isospin-dependent part of the particle-hole interaction. In the following, we used the generalized Landau-Migdal interaction of Li and Klemt<sup>6</sup> which includes in addition to the zero-range terms also the one-pion- and one- $\rho$ -exchange potentials explicitly. The isospin-dependent part of this interaction has the form

$$\begin{aligned} F^{p-h}(r_1, r_2) = & C_0 (\tilde{f}_0' \vec{\tau}_1 \cdot \vec{\tau}_2 + \tilde{g}_0' \vec{\sigma}_1' \cdot \vec{\sigma}_2 \vec{\tau}_1 \cdot \vec{\tau}_2) \delta(\vec{r}_1 - \vec{r}_2) \\ & - f_{\pi}{}^2 \cdot m_{\pi} [h_2^{(1)}(im_{\pi} r) \exp(-m_{\pi} r) S_{12}(\Omega) + \frac{1}{3} \vec{\sigma}_1 \cdot \vec{\sigma}_2 \exp(-m_{\pi} r) / m_{\pi} r] \vec{\tau}_1 \cdot \vec{\tau}_2 \\ & - f_{\rho}{}^2 \cdot m_{\rho} [-h_2^{(1)}(im_{\rho} r) \exp(-m_{\rho} r) S_{12}(\Omega) + \frac{2}{3} \vec{\sigma}_1 \cdot \vec{\sigma}_2 \exp(-m_{\rho} r) / m_{\rho} r] \vec{\tau}_1 \cdot \vec{\tau}_2. \end{aligned} \quad (2)$$

Here  $\tilde{f}_0'$  and  $\tilde{g}_0'$  are the zero-order Migdal parameters, corrected for the contributions of the direct ( $g'^{\text{dir}}$ ) and exchange ( $g'^{\text{exch}}$ ) terms of the one-pion-exchange potential (OPEP) and  $\rho$ -exchange potential<sup>6</sup>

$$\tilde{g}_0' = g_0' - g_{\pi}{}^{\text{dir}} - g_{\rho}{}^{\text{dir}} - \frac{1}{4}(g_{0\pi}{}^{\text{exch}} + g_{0\rho}{}^{\text{exch}}), \quad (2a)$$